Nuclear Engineering and Technology 55 (2023) 1476–1484

Contents lists available at ScienceDirect

Nuclear Engineering and Technology

journal homepage: www.elsevier.com/locate/net

Original Article

Geochemical and S isotopic studies of pollutant evolution in groundwater after acid in situ leaching in a uranium mine area in Xinjiang

Zhenzhong Liu [a], Kaixuan Tan [a, **], Chunguang Li [a, b, c, *], Yongmei Li [a, b], Chong Zhang [a, d], Jing Song [a], Longcheng Liu [b, c, e]

[a] School of Resource Environment and Safety Engineering, University of South China, Hengyang, 421001, PR China
[b] R&D Center of Radioactive Waste Treatment, Disposal and Modeling, University of South China, Hengyang, 421001, PR China
[c] China Institute of Atomic Energy, Beijing, 102413, PR China
[d] Beijing Research Institute of Chemical Engineering Metallurgy, Beijing, 101149, PR China
[e] Department of Chemical Engineering, Royal Institute of Technology, Stockholm, Sweden

ARTICLE INFO

Article history:
Received 5 September 2022
Received in revised form
2 November 2022
Accepted 6 December 2022
Available online 14 December 2022

Keywords:
Acid in situ leaching of uranium
Pollution evolution
Sulfate elimination
Sulfur isotopes analysis

ABSTRACT

Laboratory experiments and point monitoring of reservoir sediments have proven that stable sulfate reduction (SSR) can lower the concentrations of toxic metals and sulfate in acidic groundwater for a long time. Here, we hypothesize that SSR occurred during in situ leaching after uranium mining, which can impact the fate of acid groundwater in an entire region. To test this, we applied a sulfur isotope fractionation method to analyze the mechanism for natural attenuation of contaminated groundwater produced by acid in situ leaching of uranium (Xinjiang, China). The results showed that $\delta^{34}S$ increased over time after the cessation of uranium mining, and natural attenuation caused considerable, area-scale immobilization of sulfur corresponding to retention levels of 5.3%–48.3% while simultaneously decreasing the concentration of uranium. Isotopic evidence for SSR in the area, together with evidence for changes of pollutant concentrations, suggest that area-scale SSR is most likely also important at other acid mining sites for uranium, where retention of acid groundwater may be strengthened through natural attenuation. To recapitulate, the sulfur isotope fractionation method constitutes a relatively accurate tool for quantification of spatiotemporal trends for groundwater during migration and transformation resulting from acid in situ leaching of uranium in northern China.

1. Introduction

Acid in situ leaching of uranium (AISLU) is a widely applied underground mining method in which U is recovered via oxidative dissolution of sandstone-hosted U ore deposits by injection and pumping, since it does not produce tailings and is suitable for low-grade ores [1,2]. The AISL mining process, however, generates mobilizable SO_4^{2-} and U(VI), which may potentially pollute the groundwater downgradient of ISL mines when advected by groundwater after mining ceases [3]; this may pose hazards to human health and ecosystem stability [4]. Acid mine drainage management in Australia is estimated to cost over 500 million USD per year for retired mine sites [5,6]; thus, the economic and environmental impacts of acid mine drainage have encouraged strategic development of remediation solutions [7]. The dissolved uranium concentration forms a challenge because it can bounce after repair when U(VI) generated during mining is desorbed from mineral surfaces; however, U(VI) is expected to be stably encapsulated by sulfide minerals formed during the reduction process [8]. China is rapidly expanding its nuclear power plants and needs an increasing number of uranium resources, thus promoting development of AISL and producing a number of decommissioned sites [9]. Natural attenuation is a well-known and cost-effective priority strategy and plays an important role in demonstrating regulatory compliance, as long as it works, and research on sulfate reduction is critical [10]. Despite some research, the processes resulting in natural attenuation of AISL pollutants are still not fully

* Corresponding author. School of Resource Environment and Safety Engineering, University of South China, Hengyang, 421001, PR China.
** Corresponding author.
E-mail addresses: nhtkx@126.com (K. Tan), lichunguang1983@163.com (C. Li).

https://doi.org/10.1016/j.net.2022.12.009

understood [11,12]. As a result, it is difficult to assess the effectiveness of natural attenuation after uranium mining.

The AISL decommissioned uranium mine is a major U(VI) and SO_4^{2-} groundwater contamination source due to the large amounts of uranium and sulfate ions derived from AISLU production worldwide [13]. To accurately evaluate the effects of natural attenuation, it is necessary to determine the behavior and fundamental mechanism for release and removal of U(VI) and SO_4^{2-} from AISL decommissioned uranium sites under environmentally relevant conditions. Natural attenuation is complex since it involves dilution, adsorption, reduction and other processes; among them, reduction is considered the most stable process. With a determined pumping-injection flux ratio and natural flow rate, the influence of dilution on pollution migration and transformation is easily calculated by software such as PHREEQC [8]. Based on findings in the literature [14,15], readsorption of uranium can affect the longevity at contaminated sites and undergo desorption when reacting with fresh water; therefore, adsorption may only delay the migration of U(VI) and barely work for SO_4^{2-}. There exists a very extensive literature on stable removal of uranium pollution by reduction with ISL, but mainly in alkaline ISL and rarely in acid ISL [16,17]. The most recent work in microbial sulfate reduction of acid mine drainage revealed by variations in the sulfur isotope activity ratio ($\delta^{34}S$, i.e., changes in $^{34}S/^{32}S$) proved the feasibility of sulfate reduction in decommissioned sites of AISLU with sulfur isotope [18,19]. However, little research has addressed the effect of sulfate reduction on the longevity for natural attenuation of pollution in decommissioned uranium mining areas by AISL [20,21], and the variations in sulfur isotopes caused by fractionation have been ignored, although sulfur isotope fractionation is a very useful tool for indicating the reduction process in situ.

The objectives of this study were thus to (i) explore the effects of environmentally relevant factors encountered at AISL retired uranium mines on natural attenuation and (ii) investigate the mechanism for fractionation of sulfate reduction on AISL uranium recommissioning mines. Field water samples from an AISL uranium mine in Xinjiang were collected before production, during the mining process and in the recommissioning stage, and the values of pH, Eh (oxidation–reduction potential), [SO_4^{2-}] and [U(VI)] were analyzed. The values of $\delta^{34}S$ in contaminated groundwater were determined at two different recommissioning stages. The Rayleigh fractionation model was used to explore the mechanism of SO_4^{2-} conversion and U pollutant removal. Using laboratory tests, the reduced contributions of pyrite and sulfate-reducing bacteria were verified.

2. Materials and methods

2.1. Sampling

The AISL uranium site is located in Yili, Xinjiang, China, in a piedmont alluvial plain region. The uranium ore deposit at the research site is divided into two mining units: yet-to-be mined MU1 and MU2. Mining was carried out using site groundwater fortified with H_2SO_4 and the oxidant H_2O_2. We collected groundwater samples from 3 wells (J1-J3) located in unexploited unit MU1 and 15 wells (K1–K15) located in recommissioning unit MU2 at the end of AISLU mining and decommissioning. The sample locations are shown in Figs. 1 and 3 monitoring wells (J4-J6) were located in a producing area approximately 1 km southeast of unit MU2. We obtained a sediment core from the ore zone during AISLU production and decommissioning. Details of the site background are represented by the mean values of wells J1-J3. Each well was sampled to determine pH, Eh, [SO_4^{2-}], [U(VI)] and S isotopes. Prior to sampling, each well was purged for at least three well volumes or

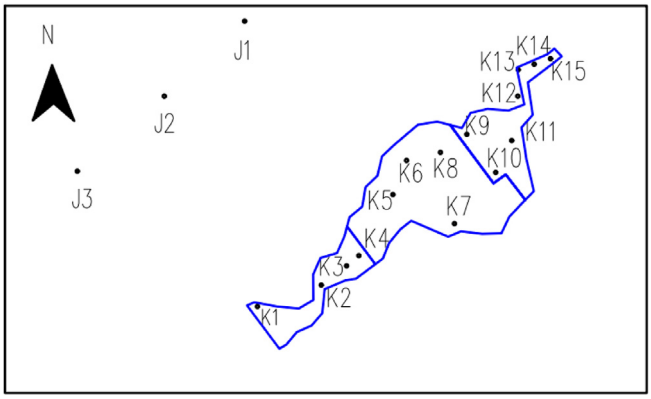

Fig. 1. Sampling locations.

until the major field parameters (temperature, pH, Eh) stabilized. Samples for cation analyses were filtered through a 0.45 μm filter membrane and then collected in precleaned PE bottles. After acidification with optimum grade HNO_3, the water samples were stored in an anaerobic glove box at room temperature until analysis. The filter membranes and the bottles were soaked in 3% dilute nitric acid for 24 h before use. The samples for anion determinations were filtered and stored in an anaerobic glove box at 4 °C without any preservative. We collected the samples for S isotope determinations as SO_4^{2-} by using the $BaCl_2$ method for precipitation of $BaSO_4$. All water samples were tested within 7 days after collection and kept sealed before detection. Ore zone sediment samples were obtained from a borehole within the MU2 area at the end of AISLU mining and decommissioning. Immediately after coring, the sediments were preserved in gas-impermeable metallized plastic bags under a N_2 atmosphere with zero-valent iron pouches as oxygen scavengers. All subsequent analyses involving the sediments were conducted under an oxygen-free atmosphere, either in a glove box or under a N_2 stream.

2.2. Water chemistry analyses

Detection of pH and Eh was completed with a pH/Eh meter (LEICI-ZDJ-48, Shanghai) immediately after water samples were obtained, and the pH/Eh meter was calibrated with a standard reagent before detection. Cation concentrations greater than 1000 ppb were determined by inductively coupled plasma–optical emission spectrometry (ICP–OES, PE Avio 220). Cation concentrations equal to or less than 1000 ppb were determined by ICP–mass spectrometry (ICP–MS, Thermal X series 2). Anionic constituents were measured by ion chromatography (IC-883, Metrohm). The RSD values of the tests with ICP–OES, ICP–MS, and IC were no more than 1%, 2%, and 3%, respectively, as given in the Supporting Information. The following tests were performed at a temperature of 20 °C.

2.3. Isotopic analyses

Sulfur isotope ratios in groundwater were measured at the Laboratory for Environmental and Sedimentary Isotope Geochemistry, Beijing Research Institute of Uranium Geology in China, with a gas isotope ratio mass spectrometer (Delta plus). Details on sample preparation and the measurement technique can be found in the publications of Brown et al. (2018) and Druhan et al. (2014). The analytical uncertainty (2σ) for the isotope measurements was 0.15‰, as determined from long-term measurements of S isotope standard NBS 127 and American standards. We report the

measured $^{34}S/^{32}S$ isotope ratios as $\delta^{34}S$ relative to that of the standard reference material, i.e., Canyon Diablo Troilite, according to

$$\delta^{34}S = \left[\frac{\left(^{34}S/^{32}S\right)_{sample}}{\left(^{34}S/^{32}S\right)_{CDT}} - 1 \right] \times 1000\,‰ \quad (2)$$

where the subscript CDT is used to denote the Canyon Diablo Troilite standard solution.

2.4. Solid-phase characterization

Microbial diversity of the sediment core was determined by metagenomic analysis, and the detailed analytical and data reduction methods can be found in Weimin et al. [22]. To assess the distribution of reducing sediment on tailings at the postmining site, postreducing uranium mining tailings were analyzed with a scanning electron microscope as well as an energy dispersive spectrometer (SEM–EDS, Phenom Pharos) under backscattered electron imaging. To assess the presence of reduced sulfide sediments in the strata, the sediment cores were analyzed by backscattered electron imaging and energy dispersive spectrometry. To reveal solid-phase Fe speciation, the sediment core was studied by X-ray photoelectron spectroscopy (XPS, Thermo Fisher 250XI), and a spin-orbit splitting of 13.1 eV and satellite peaks for Fe^{2+} and Fe^{3+} were used for fitting the Fe 2p spectra. The proportions of Fe^{2+} and Fe^{3+} were calculated from the respective peak areas [23].

3. Results and discussion

3.1. Characteristics of major pollutants during mining

The major constituents of natural groundwater are shown in Table 1, and they meet the national standard for Class III groundwater in China. The natural groundwater is in a relatively reducing condition with a pH of 8.32 and an Eh of 370 mV. The relatively reducing environment causes the U(VI) in groundwater to precipitate. Before mining, apart from the high uranium concentration (99.1 μg/L) in natural groundwater, all other ions and trace elements met the third-class groundwater standard recommended by China. During AISL mining activities, the composition of groundwater developed the values displayed in Table 2. The mean values for [SO_4^{2-}] and [U(VI)] were 16108.4 mg/L and 143.3 mg/L, respectively, which were 126 times and 1446 times the corresponding background values for groundwater. Simultaneously, the pH decreased from 8.32 to 1.37, and Eh increased from 370 mV to 657 mV.

3.2. Environmental characteristics of groundwater after decommissioning

The results for monitoring groundwater in 15 wells at the end of AISLU mining and at the stage of decommissioning are shown in Table 3 and Table 4. Similar to groundwater at the end of mining activities, the main pollutants of groundwater in the AISL uranium mine area were still SO_4^{2-}, H^+ and U(VI), and the overall groundwater environmental pollution was still serious. Tables 3 and 4 show that at the end of AISLU mining, the range for SO_4^{2-} concentration was 257–19488 mg/L, the range for U(VI) concentration was 34.9–45690 μg/L, the pH ranged from 2.37 to 8.09, and the Eh value ranged from 454 mV to 639 mV. None of the 15 wells had all pollutant concentrations below the background values. Furthermore, five years after decommissioning, the concentrations of SO_4^{2-} and U(VI) ranged from 82.0 mg/L to 16372 mg/L and 2.7 μg/L to 8976 μg/L, respectively. The pH range was 3.18–8.26, and the Eh range was 293–609 mV. As a result, the concentrations of groundwater pollutants had decreased below the background values in 5 of the 15 wells, and some values (K4, K5, K8, K10, K12, K14) even reached the national standard for Class III groundwater in China.

The overall temporal variations in groundwater pollution are shown in Table 5, which was obtained by summarizing the extreme and average concentrations of pollutants from Tables 3 and 4. Table 4 shows that the maximum, minimum and mean values for the concentrations of SO_4^{2-} and U(VI) in groundwater in the mining area had decreased significantly within 5 years after decommissioning. The maximum decreases in SO_4^{2-} and U(VI) concentrations were 69.8% and 91.3%, respectively. The mean value of pH from groundwater in 15 wells had increased greatly; additionally, the pH values for the groundwater in 9 wells were higher than the national standard for Class III groundwater in China. The mean value of Eh for the groundwater in 15 wells had decreased obviously; among them, 6 Eh values were close to or below the background value (370 mV) for the groundwater. The above data show that, after decommissioning of the AISL uranium area, the groundwater was gradually restored to a near-neutral, weakly oxidizing to reducing environment, and the concentrations of SO_4^{2-} and U(VI) gradually decreased. Therefore, the groundwater environment exhibited a certain self-purification capacity after pollution by the AISL uranium mine.

Table 1
Major composition of natural groundwater and drinking water standard.

Item	SO42- (mg/L)	pH	Eh (mV)	U(VI) (μ g/L)	δ^{34} S (‰)
JI	50.5	8.22	354	53.3	1.5
J2	243	8.46	390	135	−2.2
J3	90.5	8.28	366	109	−1.4
Mean	128	8.32	370	99.1	−0.7
China standard	≤250	6.5–8.5	–	–	–

Table 2
Major composition of groundwater during AISL mining.

Item	$SO4^{2-}$ (mg/L)	pH	Eh (mV)	U(VI) (mg/L)	δ^{34} S (‰)
J4	15080.2	1.36	655	143.4	0.2
J5	15072.9	1.34	650	142.2	1.3
J6	18172.1	1.41	666	144.4	−0.6
Mean	16108.4	1.37	657	143.3	0.3
China standard	≤250	6.5–8.5	–	–	–

Table 3
Major composition of groundwater in the end of the AISLU mining.

Item	SO_4^{2-} (mg/L)	U(VI) (μg/L)	δ^{34} S (‰)	pH	Eh (mV)
K1	10153	9853	0.1	3.05	650
K2	11141	759	−0.9	2.78	638
K3	14224	6818	0.4	3.00	623
K4	986	52.7	0.6	5.97	533
K5	643	83.5	2.7	8.09	454
K6	17113	45690	0.6	2.85	648
K7	12074	40674	−0.7	2.81	632
K8	18151	32710	0.1	2.83	639
K9	14393	29372	−0.3	3.13	578
K10	16541	29717	−0.5	3.11	583
K11	3008	1079	1.7	4.00	573
K12	257	34.9	3	7.83	476
K13	13776	5128	1.1	3.2	637
K14	19488	31683	−0.2	3.25	635
K15	18070	4691	1.2	2.37	624

Table 4
Major composition of groundwater recommissioning for 5 years.

Item	SO_4^{2-} (mg/L)	U(VI) (μg/L)	δ^{34} S (‰)	pH	Eh (mV)
K1	5276	8976	2.2	3.5	518
K2	6343	177	2.5	3.75	508
K3	3186	2195	3.2	4.18	519
K4	84.3	8.68	4	6.94	405
K5	236	11	9.6	7.48	416
K6	796	21.8	7.1	7.66	388
K7	625	220	5	7.73	380
K8	120	20.4	7.9	8.26	350
K9	5140	706	3.6	3.22	520
K10	136	2.61	5.8	7.1	402
K11	818	123	3.5	6.51	341
K12	115	6.72	5.4	7.49	337
K13	11968	2942	2.1	2.61	588
K14	82	2.74	13	7.29	293
K15	16372	3141	1.3	3.18	609

3.3. Evolution law for the groundwater environment

To investigate the mechanisms for transformations of pollutants in groundwater from the AISL uranium mining area, the variations in SO_4^{2-} and U(VI) concentrations in all wells were analyzed with Eh. Fig. 2 shows the relationship between the SO_4^{2-} concentration in groundwater and the oxidation–reduction potential value Eh. There was a positive linear correlation between [SO_4^{2-}] and Eh ($R^2 = 0.86$); that is, the concentration of SO_4^{2-} decreased with decreases in the oxidation–reduction potential value Eh for groundwater in the AISL uranium mining area. There was a relatively poorer correlation between the concentration of U(VI) and Eh ($R^2 = 0.77$) compared to that between Eh and [SO_4^{2-}], as shown in Fig. 3.

Based on the main pollutants from groundwater at the end of mining and 5 years after decommissioning of MU2, the relationship between fractional SO_4^{2-} removal and the oxidation–reduction potential difference (ΔEh) was quantitatively analyzed, and the results are shown in Fig. 4. The fraction of SO_4^{2-} removed from groundwater showed a negative linear relationship with ΔEh ($R^2 = 0.57$). The fraction (%) of SO_4^{2-} concentration removed from the groundwater increased with decreasing ΔEh. When Eh decreased by more than 250 mV, the fraction of SO_4^{2-} removed from groundwater exceeded 94%, indicating that the decrease in SO_4^{2-} concentration in groundwater seen after decommissioning of the mining area was roughly affected by the reducing environment.

On the other hand, only 53% of the points indicating the fraction (%) of U(VI) removed from groundwater in acid in situ leaching decommissioned areas were well correlated with ΔEh (mV), as shown in Fig. 5. The fraction of U(VI) removed at these points also showed a negative linear correlation with ΔEh. The fraction of U(VI) removed increased with decreasing ΔEh, indicating that part of the decrease in the U(VI) concentration was also affected by reduction.

3.4. S isotope evolution and pollutant removal mechanism

The decrease in the SO_4^{2-} concentration in groundwater after AISLU was mainly caused by three factors: supplemental dilution of

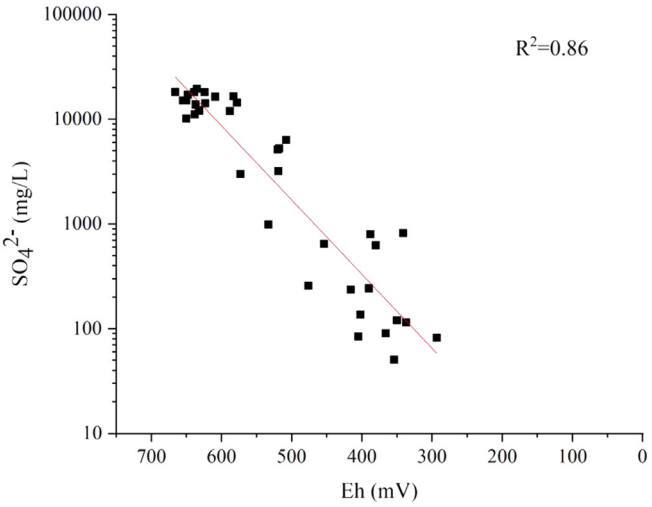

Fig. 2. Plot of SO_4^{2-} concentration vs. Eh in groundwater from AISLU mines.

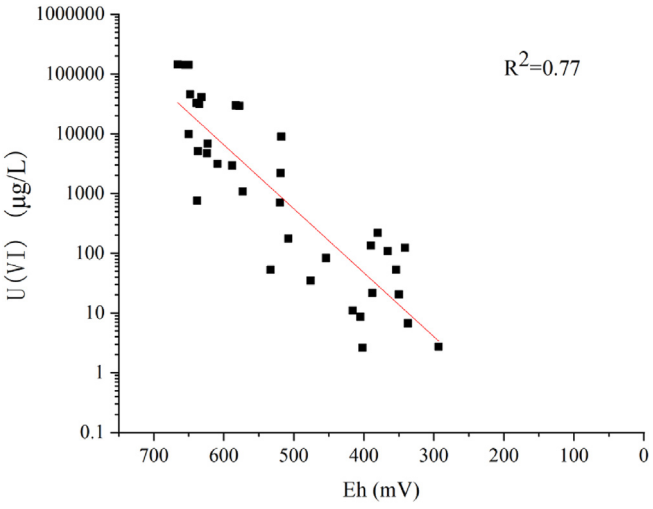

Fig. 3. Plot of U(VI) concentration vs. Eh in groundwater from AISLU mines.

fresh groundwater, precipitation of sulfate minerals (such as $CaSO_4$ and $BaSO_4$) and precipitation of reduced sulfides. It is well known that oxidation of sulfide to sulfate is a dynamic process, during which sulfur isotope fractionation is not obvious. Supplemental dilution with fresh groundwater could not induce sulfur isotope fractionation; precipitation of sulfate minerals had little effect on the fractionation of sulfur isotopes and thus can be ignored, but the biodynamic isotope fractionation effect occurring during reductive precipitation of sulfate bacteria can lead to substantial sulfur isotope fractionation [19].

During the process of sulfate reduction, ^{32}S was preferentially contained in sulfide and formed sulfide minerals (e.g., pyrite, chalcopyrite, sachtolith, and selenite), which gradually enriched

Table 5
Comparison on major composition of groundwater in the end of AISLU mining and at the stage of decommissioning.

Item	SO_4^{2-} (mg/L)			U(VI) (μ g/L)			pH			Eh (mV)		
	Minimum	Maximum	Mean	Minimum	Maximum	Mean	Minimum	Maximum	Mean	Minimum	Maximum	Mean
End of AISLU	257	19488	11335	34.9	45960	14217	2.37	8.09	3.88	454	650	595
Decommissioning	82	16372	3420	2.7	8976	1237	3.18	8.26	5.79	293	609	438

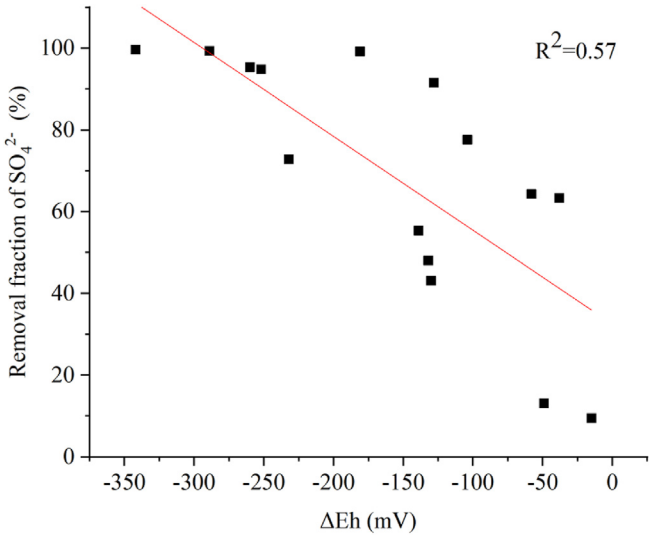

Fig. 4. Linear fit for a plot sulfate removal fraction versus ΔEh.

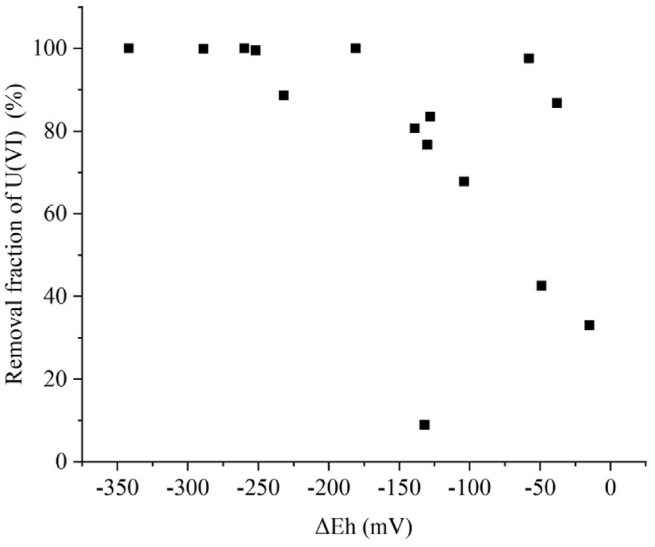

Fig. 5. Relationship between the fraction of [U(VI)] removed and ΔEh.

the remaining SO_4^{2-} in ^{34}S. The $\delta^{34}S$ value gradually increased with the extent of sulfate reduction in groundwater, and the concentration of SO_4^{2-} decreased gradually. For isotope partitioning between SO_4^{2-} and sulfides, the extent of sulfur isotope fractionation can be expressed by Eq. (3) and Eq. (4), and the processes for formation of the main sulfide minerals are shown in Eq. (5)–8.

$$^{32}SO_4^{2-} + H_2\,^{34}S f \rightarrow {}^{34}SO_4^{2-} + H_2\,^{34}S \quad (3)$$

$$\alpha SO_4^{2-} - H_2S = {}^{34}S/{}^{32}S_{SO_4^{2-}} \Big/ {}^{34}S/{}^{32}S_{H_2S} \quad (4)$$

$$2Fe^{3+} + 4H^{32}S^{-} \leftrightarrow 2Fe^{32}S_{2(s)} + 2H^{+} \quad (5)$$

$$2Pb^{2+} + 2H^{32}S^{-} \leftrightarrow 2Pb^{32}S_{(s)} + 2H^{+} \quad (6)$$

$$2Zn^{2+} + 2H^{32}S^{-} \leftrightarrow 2Zn^{32}S_{(s)} + 2H^{+} \quad (7)$$

$$Fe^{3+} + Cu^{2+} + 2H^{32}S^{-} \leftrightarrow 2FeCu^{32}S_{2(s)} + 2H^{+} \quad (8)$$

where α is the isotope fractionation factor, which describes the extent of sulfur isotope fractionation between SO_4^{2-} and H_2S. Therefore, we content that sulfur isotope fractionation is a good geochemical method with which to explore the mechanism for transformations of groundwater pollutants in acid in situ leaching uranium mining areas.

The background value for $\delta^{34}S$ in the groundwater of the unmined AISLU area was between −2.2‰ and +1.5‰, with a mean value of −0.7‰, as displayed in Table 1. During the production period of AISLU, the value of $\delta^{34}S$ ranged from −0.6‰ to +1.3‰, with a mean value of 0.3‰, due to artificial injection of sulfuric acid, as shown in Table 2. The $\delta^{34}S$ values ranged from −1.1‰ to +3.0‰, with an average of 0.36‰ at the end of AISLU mining, and this value ranged from −0.9‰ to +13‰ in the 5th year of decommissioning, with a mean of 4.47‰. The obvious increase in the $\delta^{34}S$ value for groundwater in the AISLU mining area during the decommissioning process compared to that seen at the end of production indicates that sulfur isotopes had undergone obvious fractionation after cessation of mining.

As shown in Fig. 6, the $\delta^{34}S$ value indicating the sulfur isotope composition of groundwater in the 5th year of decommissioning in the AISLU mining area was significantly higher than that in the 4th year. There was a negative correlation between the value of $\delta^{34}S$ and the concentration of SO_4^{2-} ($R^2 = 0.65$). The $\delta^{34}S$ value for the sulfur isotope composition increased significantly with decreasing SO_4^{2-} concentration. Therefore, obvious sulfur isotope fractionation occurred in the groundwater of the decommissioned AISLU mining area. With the decrease in SO_4^{2-} concentration, the extent of sulfur isotope fractionation increased, and the $\delta^{34}S$ value for the sulfur isotope composition increased.

As shown in Fig. 7, the concentration of SO_4^{2-} in groundwater was generally lower in the 5th year of decommissioning than that at the end of AISLU mining. More than 50% of the decreases in SO_4^{2-} concentrations in borehole groundwater samples were above 5000 mg/L, and the maximum decrease reached 20 g/L. There was a positive correlation between variations in the $\delta^{34}S$ value for sulfur

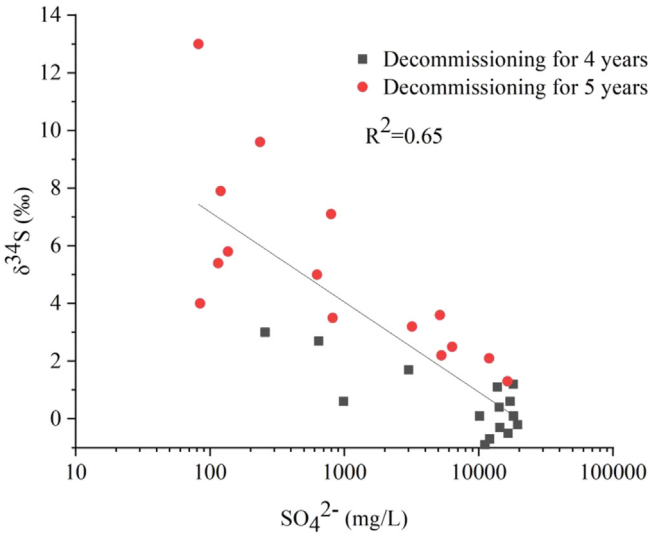

Fig. 6. Linear fit for a plot of $\delta^{34}S$ versus $[SO_4^{2-}]$.

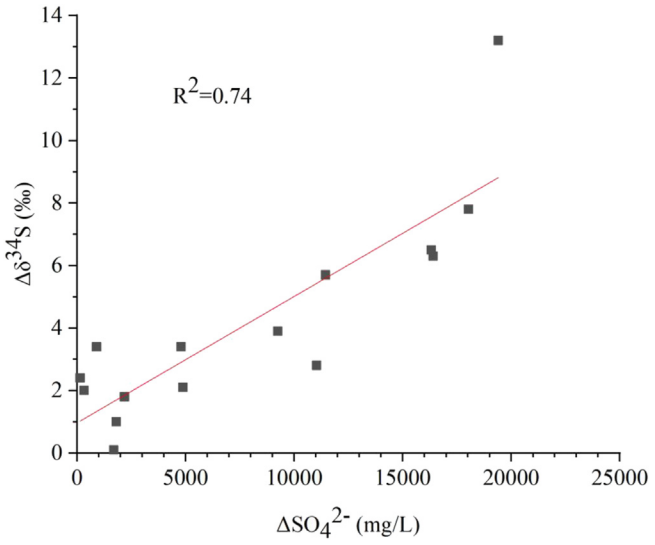

Fig. 7. Linear fit for a plot of $\Delta\delta^{34}S$ versus $\Delta[SO_4^{2-}]$.

isotope composition and the concentration of SO_4^{2-} in groundwater (R^2 = 0.74). The increment of $\delta^{34}S$ ($\Delta\delta^{34}S$) in the sulfur isotope composition increased with the growth of SO_4^{2-} concentration (i.e., ΔSO_4^{2-}). Therefore, the $\delta^{34}S$ value for groundwater in the decommissioned mining area of in situ leaching uranium mining had changed significantly, and the variation range for the $\delta^{34}S$ value increased significantly with increasing SO_4^{2-} concentration.

As shown in Fig. 8, there was no obvious linear correlation between ΔSO_4^{2-}, i.e., the change in sulfate concentration in groundwater, and ΔEh, indicating that it is not accurate to use the change in ΔEh to indicate the mechanism for reduction of SO_4^{2-} in the short term. This phenomenon may occur because there are many complicating factors in the system that affect the oxidation–reduction potential, such as metastable substances. In contrast, the change in the sulfur isotope activity ratio, i.e., $\Delta\delta^{34}S$, is a better indication of sulfate reduction.

In general, from the end of AISLU mining to a decommissioning age of 5 years, sulfur isotope fractionation appears to have been significant. The range for variations in the sulfur isotope composition $\delta^{34}S$ increased with the change in sulfate concentration, ΔSO_4^{2-}.

The extent of sulfur isotope fractionation between groundwater and rock strata can be expressed by the coefficient α for sulfur isotope fractionation. α = 1 indicates that there was no isotope fractionation between the substances, and a greater deviation of α from 1 indicates greater isotope fractionation between the two phases. Rudnicki et al. used deep-sea sediments as a closed system with which to simulate isotope fractionation in bacterial sulfate reduction at different temperatures. It was found that the value of α for the system ranged from 1.009 to 1.041, which changed with temperature and more closely approached 1 when the temperature was increased [24]. To explore the fraction of SO_4^{2-} removal caused by precipitation of sulfate reduction while noting that the deep underground temperatures of uranium deposits are approximately 15 °C, the Rayleigh fractionation model for biosulfur isotope geochemistry established by Canfield [25] was used to calculate the fraction of SO_4^{2-} removed with Eq. (9) and Eq. (10), as follows:

$$\delta^{34}S_* + 1000 = \left(\delta^{34}S_0 + 1000\right) \times f^{1-\alpha} \tag{9}$$

$$X = \frac{1-f}{1-F} \times 100\% \tag{10}$$

where $\delta^{34}S_0$ is the initial activity ratio (δ) for sulfur isotopes in the original concentration of SO_4^{2-}, $\delta^{34}S^*$ is the activity ratio (δ) for sulfur isotopes in SO_4^{2-} in groundwater after reductive precipitation occurred, f is the fraction of dissolved SO_4^{2-} in pollutants that remained in the groundwater after reduction, α is the fractionation coefficient for sulfur isotopes, which was selected as 1.020, F is the fraction of dissolved SO_4^{2-} in pollutants that remained in the groundwater after total geochemical reaction, and X is the proportion of SO_4^{2-} removal caused by reductive precipitation among all processes for removal from groundwater.

By combining the sulfur isotope composition $\delta^{34}S$ (‰) and SO_4^{2-} removal fraction (%) from groundwater in each well of the decommissioned AISLU mining area in the fourth and fifth years, the fraction of SO_4^{2-} removed by reductive precipitation was calculated with the Rayleigh fractionation formula (Eq. (3) and Eq. (4)), and the calculated results are shown in Table 6. The data in Table 6 indicate that the fractions of SO_4^{2-} removed by reduction were greater than 20% in approximately 67% of the well groundwater samples, and some were even as high as 48.3%. We suggest that addition of sulfate-reducing bacteria, organic matter or inorganic

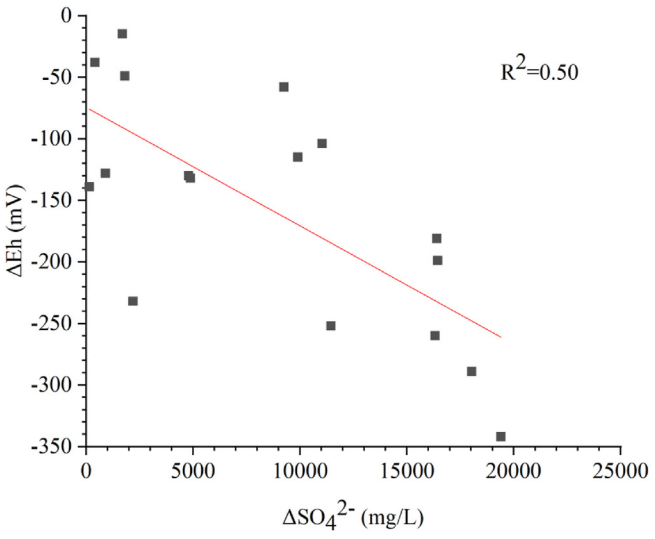

Fig. 8. Linear fit for a plot of ΔEh versus $\Delta[SO_4^{2-}]$.

Table 6
Analysis of removal effect of SO_4^{2-}.

Item	$\delta34S_{2018}$ (‰)	$\delta34S_{2019}$ (‰)	1-F (%)	1-*f* (%)	X (%)
K1	0.1	2.2	48.0	10.0	20.7
K2	−0.9	2.5	43.1	15.6	36.3
K3	0.4	3.2	77.6	13.0	16.8
K4	0.6	4	91.5	15.6	17.1
K5	2.7	9.6	63.3	29.0	45.9
K6	0.6	7.1	95.3	27.7	29.0
K7	−0.7	5	94.8	24.8	26.1
K8	0.1	7.9	99.3	32.2	32.4
K9	−0.3	3.6	64.3	17.7	27.5
K10	−0.5	5.8	99.2	27.0	27.2
K11	1.7	3.5	72.8	8.6	11.8
K12	3	5.4	55.3	11.3	20.4
K13	1.1	2.1	13.1	4.9	37.1
K14	−0.2	13	99.6	48.1	48.3
K15	1.2	1.3	9.4	0.5	5.3

Note: the value of 1-*f* is the removal fraciton of SO_4^{2-} by reduction, F is the removal fraction of SO_4^{2-} by total geochemical reaction, X is the percentage of SO_4^{2-} removal rate caused by reductive precipitation in total removal rate from groundwater.

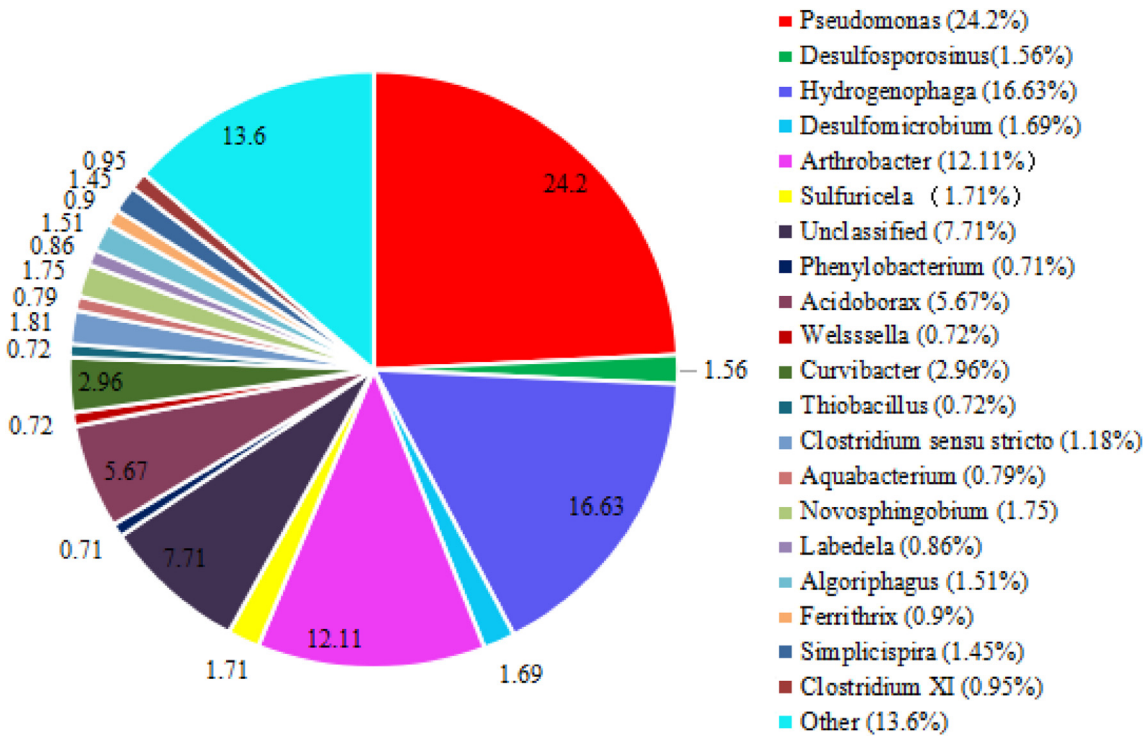

Fig. 9. Pie chart showing microbial abundance in the core samples.

reducing agents such as Na_2S and $Na_2S_2O_4$ would enhance synergistic removal of SO_4^{2-} and U(VI) from contaminated groundwater polluted by AISLU mining [26].

Based on monitoring results for the groundwater from AISLU postmining, and using the theory that the fractionation coefficient for sulfur isotopes is very small for chemical reduction fractionation but relatively large for biological reduction fractionation, reductive removal of SO_4^{2-} from groundwater in the AISLU mining area was mainly caused by microbial reduction, which provides a clearer research direction for restoration. In general, the variations in sulfur isotope compositions and the sulfur isotope fractionation model further proved that removal of SO_4^{2-} from groundwater in the AISLU mining area was mainly caused by reduction. The removal of SO_4^{2-} accompanied the removal of U(VI) and was effected by microbial reduction and precipitation, which is mainly related to reduction and precipitation by sulfate bacteria.

A microbial diversity analysis was carried out with the core samples obtained at the site, and the results are shown in Fig. 9. The core samples contained sulfate-reducing bacteria such as Desulfosporosinus (1.56%), Desulfomicrobium (1.69%) and Sulfuricela (1.71%). The emergence of the microbial sulfate reduction process during decommissioning of the AISLU mine was verified; however, some areas may need to be supplemented with sulfate-reducing bacteria. Through scanning electron microscopy and energy dispersive spectroscopy (SEM–EDS), as shown in Fig. 10, it was found that pyrite was the main sulfate-reducing mineral in the core samples formed during decommissioning and that this pyrite was combined with deposited uranium contaminants; this demonstrated that after AISLU decommissioning, sulfate contaminants can be removed through reduction while some of the uranium contaminants are precipitated.

To identify and quantify solid-phase sulfide speciation, a core sample from the AISLU decommissioned mine was analyzed by XPS. The XPS narrow spectrum analysis of Fe, which is presented in Fig. 11, shows that the core sample exhibiting overlapping peaks for the $2p_{3/2}$ and $2p_{1/2}$ Fe states. The Fe $2p_{3/2}$ satellite exhibited a binding energy peaks at 711.56 eV and 724.36 eV, which indicated that the core sample contained Fe(II). The characteristics binding energy of 714.45 eV and 727.25 mV indicated that there may be Fe(III) in the core sample. The ratio of Fe(III) to Fe(II) was approximately 1.0:1.9. Since the ideal monochromatic X-ray of the irradiated sample was not monochromatic, the conventional Kα 1,2 X-rays were mixed with slightly higher energy Kα 3, 4, 5, 6 and Kβ X-rays, which resulted in small accompanying peaks in the XPS spectra in addition to the main peak. Comparisons with the XPS database and the literature showed that the compound FeS_2 may have existed in the core sample [27]. This demonstrated that a large amount of sulfate may have been reduced in the system.

4. Conclusion

Uranium- and sulfate ion-containing groundwater is a primary source for U and SO_4^{2-} contamination in groundwater. Substantial amounts of U, SO_4^{2-} and the associated toxic metals could be mobilized from the contaminated groundwater area due to cessation of the injection and pumping production of the AISLU mine, which generates well-known ecological risks. However, previous studies mainly explored dilution and adsorption of the contaminants in groundwater from a decommissioned AISLU mine, and reduction of sulfate in actual AISLU-contaminated groundwater has rarely been studied. This study showed that a considerable amount of SO_4^{2-} in groundwater was reduced by sulfate-reducing bacteria

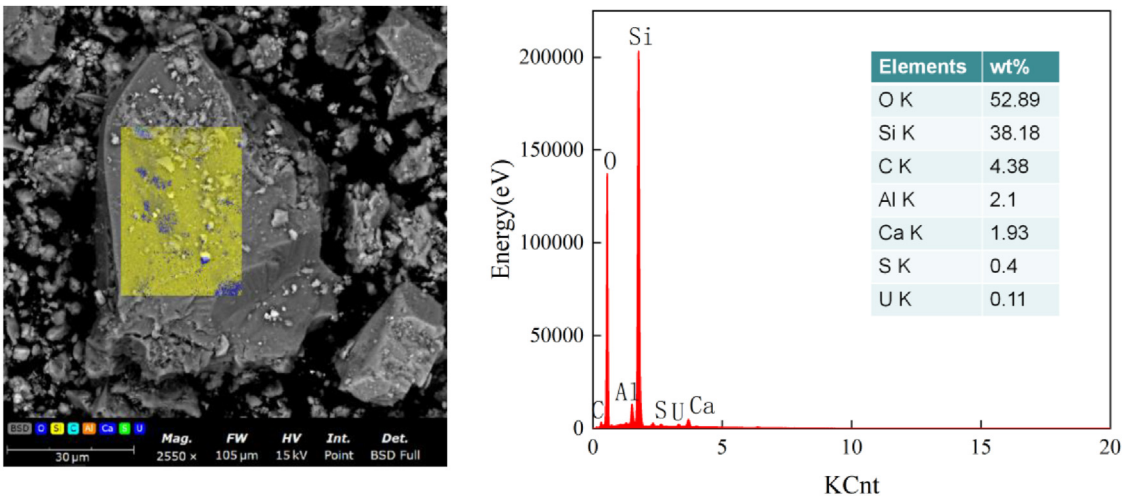

(a) End of AISLU mining.

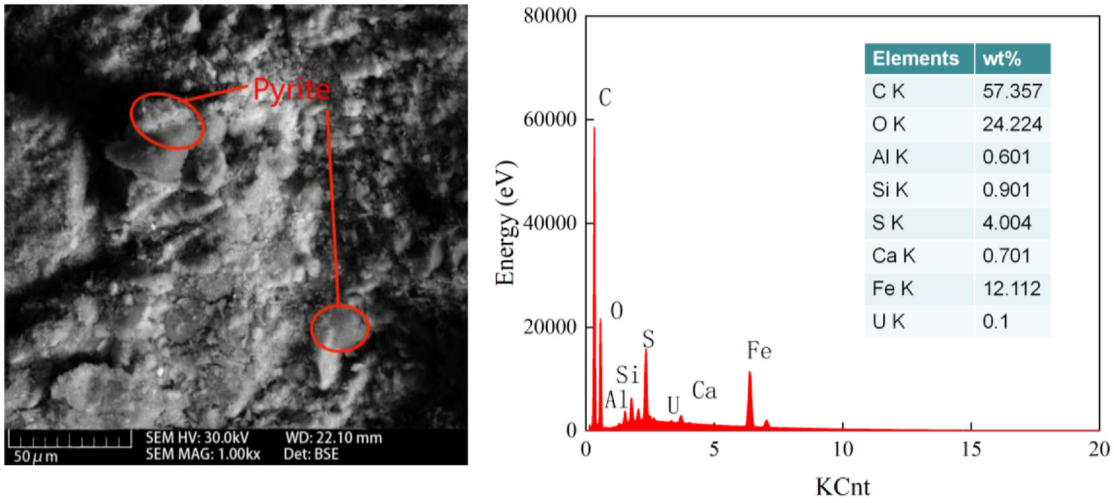

(b) During the AISLU mine decommissioning stage.

Fig. 10. SEM-EDS images of core samples.

and organic matter during AISLU mine decommissioning. The environmental hazards and ecological risks of the contaminated groundwater were naturally attenuated by SO_4^{2-} reduction and synchronous removal of U(VI), since $\delta^{34}S$ increased and SO_4^{2-} and U(VI) were converted into sulfides together. Thus, the reduction behavior and fundamental mechanism typical of SO_4^{2-} in groundwater contaminated by AISLU under environmentally relevant conditions provides an updated understanding and a more accurate assessment for in situ removal of SO_4^{2-} and U(VI) from contaminated groundwater.

High levels of SO_4^{2-} and U(VI) removal (99.6% and ~100%) were observed with groundwater from representative wells of an AISLU mine, and they were linked to natural attenuation occurring during the decommissioning process. According to our findings, there is a positive correlation between the percentage of SO_4^{2-} removed and Eh. The variation in sulfur isotope composition ($\Delta\delta^{34}S$) can be used to uncover the mechanism for reduction and removal of SO_4^{2-} in situ and predict the fraction of SO_4^{2-} reduced during removal. Moreover, our study suggests that addition of sulfate-reducing bacteria, organic matter or inorganic reducing agents, such as Na_2S and dithionite, enhances the synergistic removal of SO_4^{2-} and U(VI) from contaminated groundwater polluted by AISLU mining. These insights are helpful in developing predictive schemes for in situ decommissioning of AISLU mines.

Author contributions

Zhenzhong Liu and Tan Kaixuan conceived the idea. Yongmei Li and Jing Song performed isotopic analyses. Zhenzhong Liu, Kaixuan Tan and Chunguang Li drafted the manuscript and interpreted the data. Chong Zhang and Longcheng Liu revised the manuscript.

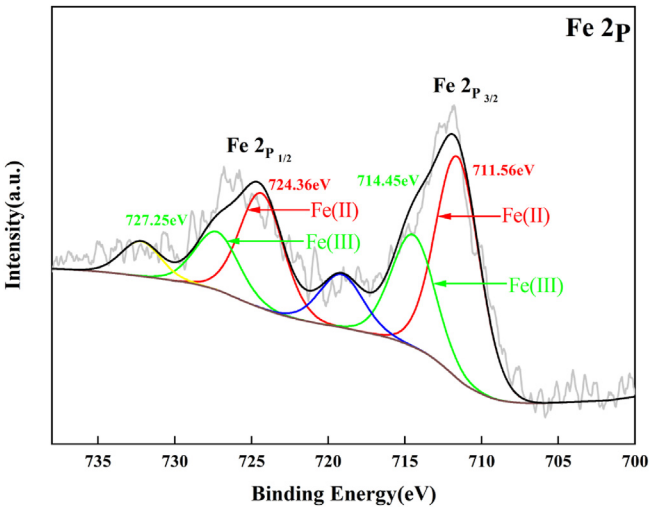

Fig. 11. Narrow sweep Fe XPS data for a core sample.

Declaration of competing interest

The authors declare that they have no known competing financial interests or personal relationships that could have appeared to influence the work reported in this paper.

Acknowledgments

This work was supported by the National Natural Science Foundation of China (U1703123), the Research Foundation of Education Bureau of Hunan Province, China (20B494), and the Natural Science Foundation of Hunan Province, China (2019JJ50496).

Appendix A. Supplementary data

Supplementary data to this article can be found online at https://doi.org/10.1016/j.net.2022.12.009.

References

[1] G. Mudd, Critical review of acid in situ leach uranium mining: 1. USA and Australia, Environ. Geol. 41 (2001) 390–403.
[2] K. Tan, C. Li, J. Liu, H. Qu, L. Xia, Y. Hu, Y. Li, A novel method using a complex surfactant for in-situ leaching of low permeable sandstone uranium deposits, Hydrometallurgy 150 (2014) 99–106.
[3] M. Seredkin, A. Zabolotsky, G. Jeffress, In situ recovery, an alternative to conventional methods of mining: exploration, resource estimation, environmental issues, project evaluation and economics, Ore Geol. Rev. 79 (2016) 500–514.
[4] N. Pa, J. Tang, D.Z. Hou, H. Lei, D.H. Zhou, J. Ding, Enhanced uranium uptake from acidic media achieved on a novel iron phosphate adsorben, Chem. Eng. J. 423 (2021), 130267.
[5] J. Harries, Acid mine drainage in Australia: its extent and potential future liability, Supervising Scientist Rep. 125 (1997).
[6] G. Naidu, S. Ryu, R. Thiruvenkatachari, Y. Choi, S. Jeong, S. Vigneswaran, A critical review on remediation, reuse, and resource recovery from acid mine drainage, Environ. Pollut. 247 (2019) 1110–1124.
[7] M. Kalin, A. Fyson, W.N. Wheeler, The chemistry of conventional and alternative treatment systems for the neutralization of acid mine drainage, Sci. Total Environ. 366 (2006) 395–408.
[8] P.W. Reimus, M.A. Dangelmayr, J.T. Clay, K.R. Chamberlain, Uranium natural attenuation downgradient of an in situ recovery mine inferred from a cross-hole field test, Environ. Sci. Technol. 53 (2019) 7483–7493.
[9] D. Shang, B. Geissler, M. Mew, et al., Unconventional uranium in China's phosphate rock: review and outlook, Renew. Sustain. Energy Rev. 140 (2021), 110740.
[10] S. Hall, Groundwater Restoration at Uranium In-Situ Recovery Mines, South Texas Coastal Plain, US Geological Survey, 2009.
[11] Y. Dong, Y. Xie, G. Li, J. Zhang, Efficient natural attenuation of acidic contaminants in a confined aquifer, Environ. Earth. 75 (2016) 595. Sci.
[12] J. Luo, Hydraulic Control and Reactive Transport Modeling for In-Situ Bioremediation of Uranium-Contaminated Groundwater, Doctoral dissertation, Stanford University, 2006.
[13] D. Lunt, P. Boshoff, M. Boylett, Z. El-Ansary, Uranium extraction: the key process drivers, J. S. Afr. Inst. Min. Metall 107 (7) (2007) 419.
[14] M. Yin, J. Sun, H. He, J. Liu, Q. Zhong, Q. Zeng, X. Huang, J. Wang, Y. Wu, D. Chen, Uranium re-adsorption on uranium mill tailings and environmental implications, J. Hazard Mater. 416 (6) (2021), 126153.
[15] D. Cui, B. Yang, H. Guo, G. Lian, J. Sun, Adsorption and transport of uranium in porous sandstone media, Earth Sci. Front. 29 (3) (2022) 217–226 (Chinese).
[16] A. Basu, S.T. Brown, J.N. Christensen, D.J. DePaolo, P.W. Reimus, J.M. Heikoop, G. Woldegabriel, A.M. Simmons, B.M. House, M. Hartmann, K. Maher, Isotopic and geochemical tracers for U(VI) reduction and U mobility at an in situ recovery U mine, Environ. Sci. Technol. 49 (2015) 5939–5947.
[17] S.T. Brown, A. Basu, J.N. Christensen, P. Reimus, J. Heikoop, A. Simmons, G. Woldegabriel, K. Maher, K. Weaver, J. Clay, D.J. DePaolo, Isotopic evidence for reductive immobilization of uranium across a roll-front mineral deposit, Environ. Sci. Technol. 50 (2016) 6189–6198.
[18] S. Fischer, J. Jarsjö, G. Rosqvist, C. Mörth, Catchment-scale microbial sulfate reduction (MSR) of acid mine drainage (AMD) revealed by sulfur isotopes, Environ. Pollut. 292 (B) (2022), 118478, https://doi.org/10.1016/j.envpol.2021.118478.
[19] C. Bonnetti, L. Zhou, T. Riegler, J. Brugger, M. Fairclough, Large S isotope and trace element fractionations in pyrite of uranium roll front systems result from internally-driven biogeochemical cycle, Geochem. Cosmochim. Acta 282 (2020) 113–132.
[20] H. Zhang, W. Yu, M. Luo, Z. X, H. W, Effects of microbes and organics in the environment on the reduction of U(VI) by pyrite, Chemistry 83 (2) (2020) 167–171 (In Chinese).
[21] Q. Zhou, K. Tan, Y. Liu, Column experimental study on restoration of polluted groundwater from in situ leaching uranium mining with Sulfate Reducing Bacteria, Min. Eng. Res. 24 (2) (2009) 75–78 (In Chinese).
[22] S. Weimin, S. Xiaoxu, M.H. Max, K. Max, L. Ling, L. Baoqin, D. Yiran, X. Rui, L. Fangbai, Identification of antimonate reducing bacteria and their potential metabolic traits by the combination of stable isotope probing and metagenomic-pangenomic analysis, Enviromental Science&Technology (2021) 55.
[23] T. Yamashita, P. Hayes, Analysis of XPS spectra of Fe^{2+} and Fe^{3+} ions in oxide materials, Appl. Surf. Sci. 254 (2008) 2441–2449.
[24] M.D. Rudnicki, H. Elderfield, B. Spiro, Fractionation of sulfur isotopes during bacterial sulfate reduction in deep ocean sediments at elevated temperatures, Geochem. Cosmochim. Acta 65 (5) (2001) 777–789.
[25] R.R. Seal, Sulfur isotope geochemistry of sulfide minerals, Rev. Mineral. Geochem. 61 (1) (2006) 633–677.
[26] J. Noah, R. Paul, H. Rose, B. Hakim, C. James, C. Kevin, Reduction and potential remediation of U(VI) by dithionite at an in-situ recovery mine: insights gained by $\delta^{238}U$, Appl. Geochem. 115 (2020), 104560.
[27] Y. Cheng, B. Arora, S.S. Şengör, et al., Microbially mediated kinetic sulfur isotope fractionation: reactive transport modeling benchmark, Comput. Geosci. 25 (2021) 1379–1391, https://doi.org/10.1007/s10596-020-09988-9.